Rhodobacter sphaeroides methionine sulfoxide reductase P reduces *R* - and *S* -diastereomers of methionine sulfoxide from a broad-spectrum of protein substrates

Lionel Tarrago, Sandrine Grosse, Marina Siponen, David Lemaire, Béatrice Alonso, Guylaine Miotello, Jean Armengaud, Pascal Arnoux, David Pignol, Monique Sabaty

Rhodobacter sphaeroides methionine sulfoxide reductase P reduces *R*- and *S*-diastereomers of methionine sulfoxide from a broad-spectrum of protein substrates

Lionel Tarrago[1,*], Sandrine Grosse[1], Marina I. Siponen[1], David Lemaire[2], Béatrice Alonso[1], Guylaine Miotello[3], Jean Armengaud[3], Pascal Arnoux[1], David Pignol[1], Monique Sabaty[1,*]

[1]Aix Marseille Univ, CEA, CNRS, BIAM, Laboratoire de bioénergétique cellulaire, Saint Paul-Lez-Durance, France F-13108; [2]Aix Marseille Univ, CEA, CNRS, BIAM, Laboratoire des Interactions Protéine-Métal, Saint Paul-Lez-Durance, France F-13108; [3]Laboratoire Innovations technologiques pour la Détection et le Diagnostic (Li2D), Service de Pharmacologie et Immunoanalyse (SPI), CEA, INRA, F-30207 Bagnols sur Cèze, France.

*Correspondence: Lionel Tarrago (lioneltarrago@msn.com) or Monique Sabaty (monique.sabaty@cea.fr)

Keywords: Enzyme kinetics, methionine sulfoxide reductase, microbiology, molybdoenzyme, oxidative stress, periplasm, protein oxidation, proteomics

Abstract

Methionine (Met) is prone to oxidation and can be converted to Met sulfoxide (MetO), which exists as *R*- and *S*-diastereomers. MetO can be reduced back to Met by the ubiquitous methionine sulfoxide reductase (Msr) enzymes. Canonical MsrA and MsrB were shown to be absolutely stereospecific for the reduction of *S*- and *R*-diastereomer, respectively. Recently, a new enzymatic system, MsrQ/MsrP which is conserved in all gram-negative bacteria, was identified as a key actor in the reduction of oxidized periplasmic proteins. The haem-binding membrane protein MsrQ transmits reducing power from the electron transport chains to the molybdoenzyme MsrP, which acts as a protein-MetO reductase. The MsrQ/MsrP function was well established genetically, but the identity and biochemical properties of MsrP substrates remain unknown. In this work, using the purified MsrP enzyme from the photosynthetic bacteria *Rhodobacter sphaeroides* as a model, we show that it can reduce a broad spectrum of protein substrates. The most efficiently reduced MetO are found in clusters of amino acid sequences devoid of threonine and proline on the C-terminal side. Moreover, *R. sphaeroides* MsrP lacks stereospecificity as it can reduce both *R*- and *S*- diastereomers of MetO, similarly to its *Escherichia coli* homolog, and preferentially acts on unfolded oxidized proteins. Overall, these results provide important insights into the function of a bacterial envelop protecting system, which should help understand how bacteria cope in harmful environments.

Abbreviations: BV, benzyl viologen; DMSO, dimethylsulfoxide; DTT, dithiothreitol; ESI-MS, Electrospray Ionization-Mass spectrometry; H_2O_2, hydrogen peroxide; HEPES4-(2-hydroxyethyl)-1-piperazineethanesulfonic acid; MES, 2-(N-morpholino)ethanesulfonic acid; MetO, methionine sulfoxide; Met-*R*-O, *R*-diastereomer of MetO; Met-*S*-O, *S*-diastereomer of MetO; MS, mass spectrometry, Msr, MetO reductase, NADPH, Nicotinamide adenine dinucleotide phosphate; NaOCl, sodium hypochlorite.

Introduction

Aerobic life exposes organisms to reactive oxygen species (ROS) derived from molecular oxygen, such as hydrogen peroxide (H_2O_2) or singlet oxygen ($^1O_2$). Bioenergetic chains are important sources of these intracellular ROS. H_2O_2, is principally produced during respiration [1] and $^1O_2$ arises from photosynthesis [2]. In most organisms, these oxidative molecules act as signaling messengers playing major roles in numerous physiological and pathological states. Furthermore, their production and elimination are tightly regulated [3]. However, numerous stresses can affect ROS homeostasis and increase their intracellular concentration to excessive values leading to uncontrolled reactions with sensitive macromolecules [4]. For instance, photosynthetic organisms, such as plants or the purple bacteria *Rhodobacter sphaeroides* can experience photo-oxidative stress in which unbalance between incident photons and photosynthetic electron transfer generate detrimental accumulation of $^1O_2$ [5]. Moreover, production of ROS could be used advantageously in a defensive strategy against potential pathogenic invaders. For instance, neutrophils produce the strong oxidant hypochlorite (ClO^-) from H_2O_2 and chlorine ions to eliminate bacteria and fungi [3]. Because of their abundance in cells, proteins are the main targets of oxidation [6]. Methionine (Met) is particularly prone to oxidation and the reaction of Met with an oxidant leads to the formation of Met sulfoxide (MetO), which exists as two diastereomers *R* (Met-*R*-O) and *S* (Met-*S*-O). Further oxidation can then lead to the formation of Met sulfone ($MetO_2$) [7,8]. As opposed to most oxidative modifications on amino acids, the formation of MetO is reversible, and oxidized proteins can be repaired thanks to methionine sulfoxide reductases (Msr) enzymes that principally exist in two types, MsrA and MsrB. These enzymes, present in almost all organisms, did not evolve from a common ancestral gene and possess an absolute stereospecificity towards their substrates. Indeed, MsrA can reduce only Met-*S*-O [7,9–12] whereas MsrB acts only on Met-*R*-O [10–14]. This strict stereospecificity was enzymatically demonstrated using chemically prepared Met-*R*-O and Met-*S*-O from racemic mixtures of free MetO or by using HPLC methods allowing discrimination of both diastereomers. A structural explanation was also provided by deciphering the mirror images of their active sites, in which only one MetO diastereomer can be accommodated [10].

While MsrA can reduce Met-*S*-O, whether as a free amino acid or included in proteins, MsrB is specialized in the reduction of protein-bound Met-*R*-O, and both are more efficient on unfolded oxidized proteins [15,16]. Eukaryotic Msrs are important actors in oxidative stress protection, aging and neurodegenerative diseases in animals [17], during environmental stresses and seed longevity in plants [18,19]. In bacteria, MsrA and MsrB are generally located in the cytoplasm [3], except in *Neisseria* or *Streptococcus* species, for which MsrA and MsrB enzymes can be addressed to the envelope [20,21]. They play a role in protecting against oxidative stress and as virulence factors [3].

Beside these stereotypical Msrs found in all kinds of organisms, several other enzymes can catalyze MetO reduction, principally in bacteria. For instance, numerous bacteria as well as unicellular eukaryotes, such as *Saccharomyces cerevisiae*, possess another type of absolutely stereospecific Msr, called free-*R*-Msr (f*R*Msr) or MsrC, which is specialized in the reduction of the free from of Met-*R*-O [22,23]. As MsrA and MsrB, the f*R*Msr uses thiol-based chemistry and the reducing power coming from NADPH to reduce its substrate [22,23].

In bacteria, several molybdenum cofactor-containing enzymes were also shown to be able to reduce oxidized Met. Particularly, the biotin sulfoxide reductase BisC, or its homolog TorZ/BisZ, specifically reduce the free form of Met-*S*-O, in the *Escherichia coli* cytoplasm and the *Haemophilus influenza* periplasm, respectively [24,25]. Moreover, *E. coli* DMSO reductase reduces a broad spectrum of substrates, including MetO [26], while the *R. sphaeroides* homolog was shown to be absolutely stereospecific towards *S*-enantiomer of several alkyl aryl sulfoxides [27]. Finally, another molybdoenzyme, MsrP (formerly known as YedY), was recently identified as a key player of MetO reduction in the periplasm [28,29]. MsrP was shown to be induced by exposure to the strong oxidant hypochlorite (ClO^-) and to reduce MetO on several abundantly present periplasmic proteins in *E. coli* [28] or on a Met-rich protein in *Azospira suillum* [29]. A most striking feature of *E. coli* MsrP (EcMsrP) is that, contrary to all known methionine sulfoxide reductases, it seems capable of reducing both Met-*R*-O and Met-*S*-O [28]. The cistron, *msrP*, belongs to an operon together with the cistron encoding the transmembrane protein MsrQ, which is responsible for the

electron transfer to MsrP from the respiratory chain. Of note, the cytosolic flavin reductase Fre was proposed as a potential alternative electron-carrier to MsrQ [30]. The operon is conserved in the genome of most gram-negative bacteria suggesting that the MsrP/Q system is very likely a key player for general protection in the bacterial envelop against deleterious protein oxidation [28,29]. *R. sphaeroides* MsrP (RsMsrP) shares 50% of identical amino acid residues with EcMsrP and transcriptomic analyses evidenced that *RsmsrP* is strongly induced under high-light conditions, suggesting a putative role in protecting the periplasm against $^1O_2$ [31].

In this paper, we describe the biochemical characterization of RsMsrP regarding its substrate specificity. Using kinetic activity experiments and mass spectrometry analysis, we show that RsMsrP is a very efficient protein-bound MetO reductase, which lacks stereospecificity and preferentially acts on unfolded oxidized proteins. Proteomic analysis indicates that it can reduce a broad spectrum of proteins in the *R. sphaeroides* periplasm, and that Met sensitive to oxidation and efficiently reduced by RsMsrP are found in clusters and in specific amino acids sequences.

Material and methods

Production and purification of recombinant proteins

Recombinant MsrP was produced similarly to the previously described protocol [32]. Briefly, *R. sphaeroides* f sp. *denitrificans* IL106 *dmsA*$^-$ strain carrying the pSM189 plasmid for production of a periplasmic MsrP with a 6-His N-terminal tag was grown in 6-liter culture under semi-aerobic conditions in Hutner medium until late exponential phase. The periplasmic fraction was extracted and loaded on a HisTrap column (GE Healthcare), MsrP was then eluted by an imidazole step gradient. MsrP solution was concentrated using 15-ml Amicon® Ultra concentrators with 10-kDa cutoff (Millipore), desalted with Sephadex G-25 in PD-10 Desalting Columns (GE Healthcare). The protein concentration was adjusted to 1 $mg.ml^{-1}$ in 30 mM Tris-HCl pH 7.5, 500 mM NaCl, the Tobacco Etch Virus (TEV) protease was added (1:80 TEV:RsMsrP mass ratio) and the solution incubated overnight at room temperature to remove the polyhistidine tag. Untagged RsMsrP was purified on a second HisTrap column, then concentrated and desalted in 50 mM 4-(2-hydroxyethyl)-1-piperazineethanesulfonic acid (HEPES) pH 8.0. Protein solution was then loaded on a Superdex™ 200 10/30 gel filtration column equilibrated with 30 mM Tris-HCl pH 7.5. Main fractions were pooled and applied to a MonoQ™ 4.6/100 PE (GE Healthcare). RsMsrP was then eluted using a linear NaCl gradient (0 to 500 mM). Fractions were analyzed on SDS-PAGE using NuPAGE™, 10 % Bis-Tris gels with MES-SDS buffer (ThermoFisher). Recombinant MsrA, MsrB, Thioredoxin Reductase (TR) 1, Thioredoxin 1 (Trx1) from *Saccharomyces cerevisiae* with polyhistidine tags, as well as the glutathione-S-transferase (GST) from *Schistosoma japonicum*, were produced and purified as previously described [15]. Protein concentrations were determined spectrophotometrically using specific molar extinction coefficients at 280 nm: 6-His-RsMSRP, 56,380 $M^{-1}.cm^{-1}$; untagged RsMsrP, 54,890 $M^{-1}.cm^{-1}$; MsrA, 34,630 $M^{-1}.cm^{-1}$; MsrB, 24,325 $M^{-1}.cm^{-1}$; TR1, 24,410 $M^{-1}.cm^{-1}$; Trx1, 9,970 $M^{-1}.cm^{-1}$; GST, 42,860 $M^{-1}.cm^{-1}$, bovine β-casein (Sigma-Aldrich), 11,460 $M^{-1}.cm^{-1}$ and chicken lysozyme (Sigma-Aldrich), 32,300 $M^{-1}.cm^{-1}$. Protein solutions were stored at -20°C until further use.

Peptides

Ser-Met(O)-Ser, QWGAGM(O)QAEED and TTPGYM(O)EEWNK peptides were obtained from GenScript® (Hong-Kong).

Preparation of oxidized bovine β-casein and its Met-R-O and Met-S-O containing counterparts

For oxidation, bovine β-casein was prepared in Phosphate Buffered Saline (PBS) at 1 $mg.ml^{-1}$ in the presence of 200 mM H_2O_2 and incubated overnight at room temperature. H_2O_2 was removed by desalting using a PD-10 column and the protein solution was concentrated with 10-kDa cutoff Amicon® Ultra concentrator. Oxidized GST was similarly prepared using 100 mM H_2O_2. To prepare Met-*R*-O containing β-casein, a solution of oxidized β-casein was incubated in 30 mM Tris-HCl pH 8 at a final concentration of 6.5 $mg.ml^{-1}$ (260 µM) in the presence of 25 mM dithiothreitol (DTT) with 10 µM MsrA and incubated overnight at room temperature. The solution was diluted 10-fold in 30 mM Tris-HCl pH 8 and passed over a HisTrap column to remove the his-tagged MsrA. After concentration, the DTT was removed by desalting using a PD-10 column. Met-*S*-O containing β-casein was prepared similarly replacing the MsrA by the MsrB (14 µM). The protein solutions were concentrated with a 10-kDa cutoff Amicon® Ultra concentrator and the final concentration was determined spectrophotometrically. Protein solutions were stored at -20°C until further use.

Enzymatic activity and apparent stoichiometry measurements

RsMsrP reductase activity was measured as described in ref. [32] with a few modifications. Benzyl viologen (BV) was used as an electron donor and its consumption was followed at 600 nm using an UVmc1® spectrophotometer (SAFAS Monaco) equipped with optic fibers in a glovebox workstation (MBRAUN Labstar) flushed with nitrogen. We determined the specific molar extinction coefficient of benzyl viologen at 8,700 $M^{-1}.cm^{-1}$ in 50 mM 2-(*N*-morpholino)ethanesulfonic acid (MES), pH 6.0 buffer. Each reaction mixture (1 ml or 0.5 ml) contained 0.2 mM BV reduced with sodium dithionite, and variable concentrations of substrates in 50 mM MES, pH 6.0 buffer.

Reactions were started by the addition of RsMsrP enzyme (10 to 46 nM). Reduction of MetO rates were calculated from the $\Delta A_{600\ nm}$ slopes respecting a stoichiometry of 2 (2 moles of BV are oxidized for 1 mole of MetO reduced). Thus, the activity values presented as k_{cat} or k_{obs} (s^{-1}) represent the number of moles of MetO reduced per mole of enzyme per second.

The apparent stoichiometry was determined similarly, using subsaturating concentrations of substrates: 1–10 µM oxidized β-casein, 1–10 µM Met-*R*-O containing β-casein and 1.5–15 µM Met-*S*-O containing β-casein. The amount of oxidized BV was determined 1 hour after the addition of the RsMsrP (46 nM) by subtracting the final A_{600} nm value from the initial one. Controls were done without the RsMsrP enzyme, or without the MetO-containing substrate. Quantities of MetO reduced were plotted as a function of substrate quantities and the apparent stoichiometry was obtained from the linear regression slope.

MsrA and MsrB activities were measured following the spectrophotometrical consumption of NADPH at 340 nm using the thioredoxin system similarly to the previously described protocol [15]. A 500-µl reaction cuvette contained 200 µM NADPH, 2 µM TR1, 25 µM Trx1 and 5 µM MsrA or MsrB and 100 µM oxidized β-casein. Production of Met was calculated respecting a stoichiometry of 1 (1 mole of NADPH is oxidized for 1 mole of Met produced).

Analysis and kinetics parameters determination were done using GraphPad® Prism 4.0 software (La Jolla, CA, USA).

Electrospray ionization/Mass spectrometry analysis of purified proteins

For oxidation, bovine β-casein (5 $mg.ml^{-1}$) in 50 mM HEPES, pH 7.0, was incubated overnight at room temperature with H_2O_2 (50 mM). H_2O_2 was removed by desalting using a PD-10 column and the protein solution was concentrated with a 10-kDa cutoff Amicon® Ultra concentrator. Oxidized β-casein (100 µM) was reduced by addition of 44 nM MsrP in a reaction mixture containing 50 mM HEPES pH 7.0, 0.8 mM BV and 0.2 mM sodium dithionite. After two hours of reaction in the glove-box, the repaired β-casein was analyzed by electrospray ionization/mass spectrometry in comparison to non-oxidized and oxidized β-casein. Analyses were performed on a MicroTOF-Q Bruker (Wissembourg, France) with an electrospray

ionization source. Samples were desalted in ammonium acetate buffer (20 mM) and concentrated with a 30-kDa cutoff Amicon® Ultra concentrator prior to analyses. Samples were diluted in CH_3CN/H_2O (1/1-v/v), 0.2% Formic Acid (Sigma). Samples were continuously infused at a flow rate of 3 µL.min^{-1}. Mass spectra were recorded in the 50-7000 mass-to-charge (*m/z*) range. MS experiments were carried out with a capillary voltage set at 4.5 kV and an end plate off set voltage at 500 V. The gas nebulizer (N2) pressure was set at 0.4 bars and the dry gas flow (N2) at 4 L.min^{-1} at a temperature of 190 °C. Data were acquired in the positive mode and calibration was performed using a calibrating solution of ESI Tune Mix (Agilent) in CH_3CN/H_2O (95/5-v/v). The system was controlled with the software package MicrOTOF Control 2.2 and data were processed with DataAnalysis 3.4.

Generation of *R. sphaeroides* 2.4.1 *msrP*$^-$ mutant

The *msrPQ* operon was amplified from *R. sphaeroides* 2.4.1 genomic DNA with the primers 5'-AGATCGACACGCCATTCACC-3' and 5'-TCGGTGAGGCGCTATCTAGG-3'. The 2.2 kb PCR product was cloned into pGEMT Easy (Promega). An omega cartridge encoding resistance to streptomycin and spectinomycin [33] was then cloned into the *BamHI* site of *msrP*. The resulting plasmid was digested with *SacI* and the fragment containing the disrupted *msrP* gene was cloned into pJQ200mp18 [34]. The obtained plasmid, unable to replicate in *R. sphaeroides*, was transferred from *E. coli* by conjugation. The occurrence of a double-crossing over event was confirmed by PCR and absence of the protein from the SDS-PAGE profile.

Preparation of periplasmic samples for proteomics analysis

R. sphaeroides 2.4.1 *msrp*$^-$ mutant was grown under semi-aerobic conditions. Periplasmic extract was prepared as previously described [32] by cells incubation in 50 mM HEPES pH 8.0, 0.45 M sucrose, 1.3 mM Ethylenediaminetetraacetic acid (EDTA) and 1 mg.ml^{-1} chicken lysozyme. For Met oxidation, the periplasmic extract (0.7 mg.ml^{-1}) was incubated with 20 mM *N*-Ethylmaleimide (NEM) and 2 mM NaOCl (Sigma-Aldrich) in 50 mM HEPES pH 8.0, 50 mM NaCl for 10 min at room temperature. NaOCl was

removed by desalting using a PD-10 column and buffer was changed to 50 mM MES pH 6.0. The protein solution was concentrated with a 3-kDa cutoff Amicon® Ultra concentrator. Three reaction mixtures were prepared in the glove box containing 35 µl of periplasmic extract, 1 mM benzyl viologen, 2 mM dithionite in 50 mM MES pH 6.0. The protein concentration in each reaction was 2.5 $mg.ml^{-1}$. The first reaction contained non-oxidized periplasmic extract, the second and third ones contained oxidized periplasmic extract. For the third reaction (repaired periplasm) 10 µM RsMsrP was added. The reactions were incubated for three hours at room temperature.

Trypsin proteolysis and tandem mass spectrometry

Protein extracts were immediately subjected to denaturing PAGE electrophoresis for 5 min onto a 4–12% Bis-Tris gradient 10-well NuPAGE™ gel (Thermofisher). The proteins were stained with Coomassie Blue Safe solution (Invitrogen). Polyacrylamide bands corresponding to the whole proteomes were sliced and treated with iodoacetamide followed by trypsin as previously recommended [35]. Briefly, each band was destained with ultra-pure water, reduced with DTT, treated with iodoacetamide, and then proteolyzed with Gold Mass Spectrometry Grade Trypsin (Promega) in the presence of 0.01% ProteaseMAX surfactant (Promega). Peptides were immediately subjected to tandem mass spectrometry as previously recommended to avoid methionine oxidation [36]. The resulting peptide mixtures were analyzed in a data-dependent mode with a Q-Exactive HF tandem mass spectrometer (Thermo) coupled on line to an Ultimate 3000 chromatography system chromatography (Thermo) essentially as previously described [37]. A volume of 10 µL of each peptide sample was injected, first desalted with a reverse-phase Acclaim PepMap 100 C18 (5 µm, 100 Å, 5 mm x 300 µm i.d., Thermo) precolumn and then separated at a flow rate of 0.2 $\mu L.min^{-1}$ with a nanoscale Acclaim PepMap 100 C18 (3 µm, 100 Å, 500 mm x 300 µm i.d., Thermo) column using a 150 min gradient from 2.5 % to 25 % of CH_3CN, 0.1% formic acid, followed by a 30 min gradient from 25% to 40% of CH_3CN, 0.1% formic acid. Mass determination of peptides was done at a resolution of 60,000. Peptides were then selected for fragmentation according to a Top20 method with a dynamic

exclusion of 10 sec. MS/MS mass spectra were acquired with an AGC target set at 1.7 10^5 on peptides with 2 or 3 positive charges, an isolation window set at 1.6 *m/z*, and a resolution of 15,000.

MS/MS spectrum assignment, peptide validation and protein identification

Peak lists were automatically generated from raw datasets with Proteome Discoverer 1.4.1 (Thermo) and an in-house script with the following options: minimum mass (400), maximum mass (5,000), grouping tolerance (0), intermediate scans (0) and threshold (1,000). The resulting .mgf files were queried with the Mascot software version 2.5.1 (Matrix Science) against the *R. sphaeroides* 241 annotated genome database with the following parameters: full-trypsin specificity, up to 2 missed cleavages allowed, static modification of carbamidomethylated cysteine, variable oxidation of methionine, variable deamidation of asparagine and glutamine, mass tolerance of 5 ppm on parent ions and mass tolerance on MS/MS of 0.02 Da. The decoy search option of Mascot was activated for estimating the false discovery rate (FDR) that was below 1%. Peptide matches with a MASCOT peptide score below a P value of 0.05 were considered. Proteins were validated when at least two different peptides were detected. The FDR for proteins was below 1% as estimated with the MASCOT reverse database decoy search option.

Ice logo analysis

Ice logo analysis were performed using the IceLogo server (http://iomics.ugent.be/icelogoserver/index.html) [38].

Results

The *R. sphaeroides* MsrP is an efficient protein-MetO reductase

The results showing that the EcMsrP is a protein-bound MetO reductase, able to reduce both *R*- and *S*-diastereomer of MetO [28] prompted us to evaluate whether these properties are conserved for RsMsrP. As the EcMsrP was determined to be 5-fold less efficient in reducing the Met-*S*-O than Met-*R*-O, and knowing that all previously identified MetO reductases were absolutely stereospecific towards one enantiomer, we thought that it cannot be excluded that a protein contamination might explain the apparent ability of the EcMsrP to reduce the Met-*S*-O [28]. Such potential Met-*S*-O reductase contaminant should be able to use benzyl viologen (BV) as electron provider in activity assays and a good candidate is the periplasmic DMSO reductase [26,27]. Thus, we prepared the recombinant RsMsrP from a *R. sphaeroides* strain devoid of the *dorA* gene encoding the catalytic subunit of the DMSO reductase [32]. After purification on Ni-affinity column and removal of the polyhistidine tag, the mature enzyme was purified by gel filtration, followed by strong anion exchange, yielding a highly pure enzyme (Supplementary Figure S1).

After optimal pH determination showing that RsMsrP acts efficiently between pH 5.5 and 8.0 (Supplementary Figure S2), we determined the kinetic parameters of RsMsrP using BV as an electron provider and several model substrates: the free amino acid MetO, a synthetic tripeptide Ser-MetO-Ser and the oxidized bovine β-casein (Table 1). The β-casein contains 6 Met, it is intrinsically disordered, and was shown as an efficient substrate for the yeast MsrA and MsrB, after oxidation [15] (see also Supplementary Figure S3). Commercial β-casein contains a mixture of genetic variants, appearing as multiple peaks on mass spectrometry (MS) spectra (Figure 1A). After oxidation with H_2O_2, MS analysis confirmed an increase in mass of 96 Da for each peak, very likely corresponding to the addition of 6 oxygen atoms on the Met residues (Figure 1B). Using the free MetO, we determined a k_{cat} of ~ 122 s^{-1} and a K_m of ~ 115,000 µM, yielding a catalytic efficiency (k_{cat} /K_m) of ~ 1,000 $M^{-1}.s^{-1}$ (Table 1). With the Ser-MetO-Ser peptide, the k_{cat} and the K_m values were ~ 108 s^{-1} and ~ 13,000 µM, and thus the k_{cat}/K_m was ~ 8,300 $M^{-1}.s^{-1}$. Compared to free MetO, the ~ 8-fold increase in catalytic efficiency is due to the lower K_M, and thus this indicates that

the involvement of the MetO in peptide bonds increases its ability to be reduced by RsMsrP. With the oxidized β-casein, the k_{cat} and the K_m were ~ 100 s^{-1} and ~ 90 µM, respectively. The k_{cat}/K_m was thus ~ 1,000,000 $M^{-1}.s^{-1}$. This value, 4 orders of magnitude higher than the one determined with free MetO, indicates that the oxidized protein is a far better substrate for RsMsrP. Moreover, even assuming that all MetO in the oxidized β-casein were equal substrates for the RsMsrP and thus multiplying the K_M by 6, the catalytic efficiency obtained (~ 175,000 $M^{-1}.s^{-1}$) remained ~ 175-fold higher for the oxidized protein than for the free amino acid. These results indicate that the RsMsrP acts effectively as a protein-MetO reductase.

RsMsrP reduces both Met-*R*-O and Met-*S*-O of an oxidized model protein

To determine whether the RsMsrP can reduce both MetO diastereomers, we chose the oxidized bovine β-casein as a model substrate because it was efficiently reduced by the yeast MsrA and MsrB indicating the presence of both *R* and *S* diastereomers of MetO [15]. After oxidation with H_2O_2, we treated the protein with MsrA and MsrB, taking advantage of their stereospecificity, to obtain protein samples containing only the Met-*R*-O (*"β-casein*-R-*O"*) or the Met-*S*-O (*"β-casein*-S-*O"*), respectively. The absence of one or the other diastereomer of MetO was validated by the absence of remaining Msr activity (Supplementary Figure 3). These three forms, containing either two or only one diastereomer of MetO, were tested as substrate for RsMsrP (Figure 2). We measured a k_{cat} of ~ 45 s^{-1} with the oxidized β-casein, which decreased to ~ 30 and to 5 s^{-1} for the β-casein containing the *R* or the *S* sulfoxide, respectively. This result shows that RsMsrP can reduce both diastereomers of MetO, but appears 6-fold less efficient to reduce Met-*S*-O than Met-*R*-O.

From this result, we postulated that RsMsrP should be able to reduce all MetO in the oxidized β-casein, as this protein was intrinsically disordered and thus all MetO were very likely accessible. We evaluated this hypothesis by mass spectrometry analysis. When incubated with RsMsrP, the mass of the oxidized protein decreased by 96 Da, showing that all MetO were reduced (Figure 1C). Altogether, these results clearly showed that RsMsrP was able to reduce both *R*- and *S*-diastereomers of MetO contained in the oxidized β-casein, and thus lacked stereospecificity.

The RsMsrP preferentially reduces Met-*R*-O but acts effectively on Met-S-O too

To gain insight into the substrate preference of RsMsrP toward one of the diastereomers of MetO, we performed kinetics analysis using the oxidized β-casein containing the *R* or *S* diastereomers of MetO (Table 1; Supplementary Figure S4). With the protein containing only the *R*-diastereomer of MetO (*"β-casein*-R-*O"*), we determined a k_{cat} of ~ 50 s^{-1}, a K_m of ~ 50 µM and thus a catalytic efficiency of ~ 950,000 $M^{-1}.s^{-1}$. In the case of the protein containing only the Met-*S*-O (*"β-casein*-S-*O"*), the k_{cat} and K_m were ~ 8 s^{-1} and of ~ 50 µM, respectively. This yielded a catalytic efficiency of 142,000 $M^{-1}.s^{-1}$. This value, ~ 7 fold lower than the one obtained with the β-casein-*R*-O, was due to the lower k_{cat} as the K_m was not changed. These values seem to indicate that the RsMsrP preferentially reduced the *R* than the *S* diastereomer of MetO in the oxidized β-casein. However, as we could not exclude that the proportion of Met-*R*-O was higher than the proportion of Met-*S*-O in the protein, we developed an assay to estimate the number of MetO reduced by RsMsrP in the three forms of oxidized β-casein. We measured the total moles of BV consumed for the reduction of all MetO using subsaturating concentrations of the oxidized protein. Practically, the absorbance at 600 nm was measured before and 90 min after substrate addition. As two moles of BV are consumed per mole of MetO reduced, we obtained the apparent stoichiometry of RsMsrP toward the oxidized protein by performing a linear regression on the straight part of the line and taking the slope, which defines the amount of MetO reduced as a function of substrate concentration (Figure S5). The values determined were ~ 4.6, ~ 3.2 and ~ 1.8 for the oxidized β-casein, the β-casein-*R*-O and the β-casein-*S*-O, respectively. In the case of the oxidized β-casein, we expected a value of 6 based on the data obtained by mass spectrometry (Figure 1). This may have been due to the heterogeneity of the oxidized β-casein (all Met were not initially fully oxidized) and/or to a too short time of incubation (all MetO were not fully reduced, as indicated by the presence of a peak corresponding to a portion of β-casein not fully reduced in Figure 1C). To compare the catalytic parameters, the data was normalized by multiplying the K_m by the apparent stoichiometries, yielding values per reduced MetO, thereby allowing the removal of variation due to the different numbers of reduced Met-*R*-O or Met-*S*-O. The catalytic efficiencies were thus 230,000, 300,000 and 80,000 $M^{-1}.s^{-1}$ for the oxidized β-casein, the β-casein-*R*-O and the β-casein-*S*-O, respectively

(Table 1). The highest value was that obtained for the β-casein containing only the *R* form of MetO, indicating that this diastereomer was the preferred substrate for RsMsrP. However, the value obtained with the β-casein-*S*-O was only less than 4-fold lower, showing that RsMsrP can also act effectively on the Met-*S*-O.

RsMsrP can reduce a broad spectrum of periplasmic proteins

To identify potential periplasmic substrates of RsMsrP and gain insight into its substrate specificity, we applied a high-throughput shotgun proteomic strategy. Periplasmic proteins from the *msrP*$^-$ *R. sphaeroides* mutant were extracted, oxidized with NaOCl and then reduced *in vitro* with recombinant RsMsrP. Untreated periplasmic proteins, oxidized periplasmic proteins and RsMsrP-treated oxidized periplasmic proteins were analyzed by semi-quantitative nanoLC–MS/MS. All experiments were done systematically for 3 biological replicates and resulted in the identification of 362,700 peptide-to-spectrum matches. From all 11,320 individual peptide sequences, we identified 2,553 unique Met belonging to 720 proteins. The overall percentages of Met oxidation were ~ 35%, ~ 71% and ~ 40% for proteins from the periplasm extract, the oxidized periplasm extract and the RsMsrP-repaired proteins, respectively (Supplementary Table 1). This first result indicates that RsMsrP is very likely able to reduce MetO from numerous proteins and to restore an oxidation rate similar to the one of the periplasmic extract that has not undergone any oxidation.

The identification of preferential RsMsrP substrates requires the precise comparison of the oxidation state of Met residues from periplasmic proteins before and after the action of the enzyme. After tryptic digestion, since most of the Met/MetO-containing peptides were found in low abundance (*i.e.* with very low spectral counts), we focused on the proteins robustly detected in all samples. We selected the Met-containing peptides for which at least 10 spectral counts were detected in two replicates for each condition (*i.e.* untreated periplasm, oxidized periplasm and repaired oxidized periplasm) and at least 7 spectral counts were found in the third replicate. This restricted the dataset to 202 unique Met belonging to 70 proteins (Supplementary Table 2). Overall percentage of Met oxidation (calculated as the number of spectral counts for a MetO-containing peptide vs. the total number of spectral count for this peptide) varied from 2% to

87%, from 9% to 100% and from 4% to 91% in the periplasm, oxidized periplasm and repaired oxidized periplasm, respectively. Comparison of Met-O containing peptides between oxidized and RsMsrP treated samples indicates that the percentage of reduction varied from 100 % to no reduction at all. Eleven MetO were not reduced and 22 were reduced at more than 75 % (only 2 at 100 %). The percentage of reduction for the remaining majority of MetO was almost uniformly distributed between inefficient (less than 25 %) to efficient (75% or more) reduction (Figure 3A).

No clear evidence of sequence or structure characteristic arose from these 70 identified proteins, neither in term of size or in Met content (Supplementary Table 2). The periplasmic chaperone SurA, the peptidyl-prolyl cis-trans isomerase PpiA, the thiol-disulfide interchange protein DsbA, the spermidine/putrescine-binding periplasmic protein PotD and the ProX protein were previously proposed as potential substrates of EcMsrP [28]. All these proteins contain at least one MetO amongst the most efficiently reduced by RsMsrP (Supplementary Table 2), indicating that they are potential conserved substrates of the MsrP enzymes in *E. coli* and *R. sphaeroides*, and very likely in numerous other gram-negative bacteria.

The sensitivity to oxidation of the Met belonging to these 70 proteins, and their efficiency of reduction by RsMsrP show a wide range of variation, from Met highly sensitive to oxidation and efficiently reduced to Met barely sensitive to NaOCl treatment and not reduced by RsMsrP (Supplementary Table 2). Moreover, this diversity could be visible within a single protein, in which all Met may not be uniformly oxidized and reduced. For instance, the ABC transporter DdpA, along with another putative ABC transporter (Figure 3B,C), contained one of the two only MetO found to be fully reduced in the dataset (Met-230 and Met-353, respectively), although DdpA also contained the Met-243 that was neither efficiently oxidized nor reduced. This is also illustrated by the case of the peptidyl-prolyl cis-trans isomerase, which possessed the Met found to have the higher decrease in oxidation in the entire dataset (Met-172) but also a Met almost not reduced by RsMsrP (Met-190) (Figure 3D). The Met-539 of the PQQ dehydrogenase XoxF illustrates the case in which a Met was highly sensitive to NaOCl-oxidation and very efficiently reduced (Figure 3E). Twenty-one Met were oxidized at 50 % or more and reduced by 50 % or more by RsMsrP (Supplementary Table S2).

Altogether, these results show that RsMsrP can reduce a broad spectrum of apparently unrelated proteins (only 11 Met among 202 were not reduced). However, since all MetO were not reduced with similar efficiency, some structural or sequence determinants could drive the ability of MetO to be reduced by RsMsrP.

The nature of the amino acids surrounding a MetO influences the RsMsrP efficiency

Having in hand a relatively large dataset of oxidized and reduced Met prompted us to search for consensus sequences that could favor or impair the oxidation of a Met or the reduction of a MetO by RsMsrP. For all identified Met, we extracted, the surrounding 5 amino acids on the N- and C-terminal sides to obtain an 11-amino acid sequence with the considered Met centered at the 6^{th} position. As shown for bacterial MsrB [39], this length might be sufficient to encompass the amino acids in physical contact with RsMsrP during reduction. We then performed an IceLogo analysis aiming to identify whether some residues were enriched or depleted around the target Met. The principle is to compare a 'positive' dataset of peptides, to a 'negative' one [38]. To find potential consensus sequences of oxidation, we first compared all unique MetO-containing peptides from both the untreated and the NaOCl-oxidized periplasmic extracts (our positive dataset) to the theoretical *R. sphaeroides* proteome (our negative dataset). The IceLogo presented in Figure 4A shows that MetO-containing sequences were mainly depleted of His and aromatic or hydrophobic residues (Trp, Phe, Tyr, Leu, Ile) and were mainly enriched in polar or charged amino acids (Asn, Gln, Asp, Glu and Lys). This suggests that Met in a polar environment, as commonly found at the surface of proteins, are very likely more susceptible to oxidation than those located in hydrophobic environments such as those in the protein core. We then compared all these unique MetO-containing peptides to all the Met-containing peptides from the same samples (Figure 4B), and we observed that Trp, along with His, Tyr and Cys, were principally depleted around the potentially oxidized Met. Strikingly, the only amino acid significantly more abundant around an oxidized Met was another Met in position -2 and +2. These results indicate that oxidation sensitive Met might be found as clusters.

To identify potential consensus sequence favorable to MetO reduction by RsMsrP, we performed a precise comparison of the oxidation percentage before and after the action of the enzyme. We thus defined two criteria to characterize the reduction state of each Met: i) the percentage of reduction calculated using the formula described in Supplementary Table S2 and based on the comparison of the oxidation percentages in oxidized versus repaired oxidized periplasm. For instance, a Met found oxidized at 25 % in the oxidized periplasm and at 5 % in the repaired oxidized periplasm was considered enzymatically reduced at 80 %. ii) the decrease in percentage of oxidation by comparison of the 2 samples. For instance, the same Met found oxidized at 25 % in the oxidized periplasm and 5 % in the repaired extract had a decrease in the oxidation percentage of 20 %. This second criterion was used to avoid bias in which very little oxidized Met were considered as efficient substrates (*i.e.* a Met oxidized at 5 % in the oxidized periplasm extract and at 1 % in the repaired oxidized periplasm was reduced at 80 %, similarly to one passing from 100 % to 20 %, which intuitively appears as a better substrate than the previous one). We selected as efficiently and inefficiently reduced MetO those for which both criterions were higher than 50 % and lower than 10 %, respectively. Comparison of the sequences surrounding the efficiently reduced MetO to the theoretical proteome of *R. sphaeroides* showed no depletion of amino acid, but mainly enrichment of polar amino acids (Gln, Lys, and Glu) around the oxidized Met (Figure 5A). Similar analysis with the inefficiently reduced MetO indicated the enrichment of Thr and Ser in the far N-terminal positions (-5 and -4) and of a Tyr in position -2 (Figure 5B). The C-terminal positions (+ 1 to +5) were mainly enriched in charged amino acids (Gln, Lys, and Glu), similarly to efficiently reduced MetO. This apparent contradiction may indicate that the amino acids in the C-terminal position of the considered MetO did not really influence the efficiency of RsMsrP but were observed simply because of the inherent composition of the overall identified peptides. We then compared the variation of amino acids composition of the MetO-containing peptides between both datasets, using the inefficiently reduced MetO as a negative dataset (Figure 5C). The results were similar to those obtained by comparison with the entire theoretical proteome of the bacterium, *i.e*. most enriched amino acids were polar (Glu, Gln, Asp and Lys) at most extreme positions (-5, -4 and + 2 to + 5). Of note, the conserved presence of a Gly in position -1, and the presence of several other Met around the central Met. This potential

enrichment of Met around an oxidation site is consistent with the result found for the sensibility of oxidation (Figure 4B), and indicates that potential clusters of MetO could be preferred substrates for RsMsrP. We found 16 peptides containing 2 or 3 MetO, reduced at more than 25 % by RsMsrP (Supplementary Table S2). This was illustrated, for example, by the cell division coordinator CpoB which possesses two close Met residues (66 and 69) highly reduced by the RsMsrP, or by the uncharacterized protein (YP_353998.1) having 4 clusters of MetO reduced by the RsMsrP (Supplementary Table S2).

From this analysis, the only depleted amino acids appeared to be Thr and Pro in positions -4 and -3 (Figure 4C). To validate these results, we designed two peptides, QWGAGM(O)QAEED and TTPGYM(O)EEWNK, as representative of most efficiently and most inefficiently RsMsrP-reduced peptide-containing MetO, respectively. We used them as substrates to determined reduction kinetics parameters for RsMsrP (Table 1; Supplementary Figure S6). The results showed that the peptide QWGAGM(O)QAEED was efficiently reduced, with the highest k_{cat} value from all the substrates we tested (~ 480 s^{-1}) and a K_m of ~ 4,500 µM. This yielded a k_{cat}/K_m of ~ 100,000 $M^{-1}.s^{-1}$, which is 2 orders of magnitude higher than the one determined for the free MetO, and 10-fold lower than for the oxidized β-casein (Table 1). On the contrary, the peptide TTPGYM(O)EEWNK was not efficiently reduced by RsMsrP (Table 1; Supplementary Figure S6). Indeed, we could not determine the kinetic parameters as the activity value curve never reached an inflection point using concentrations as high as 5,000 µM. The maximal k_{cat} value was determined at ~ 70 s^{-1} at 5,000 µM of peptide, which is ~ 3.5-fold less than the one determined with the same concentration of the other peptide (~ 250 s^{-1}) (Supplementary Figure S6). These results are in full agreement with the proteomics analysis and confirm that the nature of the amino acids surrounding a MetO in a peptide or a protein strongly influences its ability to be reduced by RsMsrP.

The RsMsrP preferentially reduces unfolded oxidized proteins

To test whether structural determinants affect RsMsrP efficiency of MetO reduction, we compared its activity using oxidized model proteins, either properly folded or unfolded. We started with chicken lysozyme as it is a very well folded protein highly stabilized by four disulfide bonds [40]. We oxidized it

with H_2O_2 and checked its oxidation state by mass spectrometry (Supplementary Figure S7). Surprisingly, using a protocol similar to the one allowing the complete oxidation of the 6 Met of β-casein, we observed only a weak and incomplete oxidation of the protein. The major peak corresponded to the non-oxidized form and a small fraction had an increase in mass of 16 Da, likely corresponding to the oxidation of one Met. Nevertheless, we prepared from this oxidized sample, an unfolded oxidized lysozyme by reduction with dithiothreitol in 4M urea followed by iodoacetamide alkylation of cysteines, and both samples (oxidized and unfolded oxidized), were used as substrates for RsMsrP (Figure 6). We also used glutathione-*S*-transferase (GST) which possesses 9 Met and is highly structured. After oxidation with H_2O_2, GST was incubated with 4 M of the chaotropic agent urea, a concentration sufficient to induce complete unfolding of the protein [15]. For both oxidized proteins, we observed a dramatic increase in activity after unfolding. Indeed, the RsMsrP activity increased 7-fold with the unfolded oxidized lysozyme compared to the folded one, and 6-fold in the case of the unfolded oxidized GST compared to the folded oxidized GST (Figure 6). As the unfolded oxidized protein solutions of lysozyme or GST contained a substantial amount of urea, we performed controls in which the urea was added extemporaneously in the cuvette during the measurements, showing that urea did not influence the RsMsrP activity (Supplementary Figure S8).

Mass spectrometry analysis showed that the RsMsrP was able to completely reduce the oxidized lysozyme in these conditions (Supplementary Figure S7), suggesting that observed differences of repair between the folded- and unfolded-oxidized lysozyme were not due to the incapacity of RsMsrP to reduce some MetO, but were due to kinetic parameters. We thus determined the kinetics of reduction of these proteins by RsMsrP (Table 1, Supplementary Figure S8). For the oxidized lysozyme, the k_{cat} and the K_m were ~ 4 s^{-1} and ~ 900 µM, respectively. Using the unfolded oxidized lysozyme, the k_{cat} increased to ~ 7 s^{-1} and the K_m decreased to ~ 100 µM. The catalytic efficiency determined with the unfolded oxidized lysozyme was thus ~ 18-fold higher than the one determined using the oxidized lysozyme before unfolding (70,200 vs. 4,000 $M^{-1}. s^{-1}$). Similar results were obtained with GST. Indeed, with the oxidized GST, we recorded k_{cat} and K_m values of ~ 8 s^{-1} and ~ 640 µM, respectively. Whereas for the unfolded oxidized GST, the k_{cat} was slightly higher (~ 12 s^{-1}), and the K_m was ~ 6-fold lower (~ 100 µM). The catalytic efficiency was 10-fold

474 higher for the unfolded oxidized GST than for its folded counterpart (Table 1; Supplementary Figure S8).
475 Altogether, these results showed that RsMsrP is more efficient at reducing MetO in unfolded than in folded
476 oxidized proteins. Moreover, as evidenced with lysozyme that contained only one MetO in our conditions,
477 the increase in activity using unfolded substrate is not dependent on the number of MetO reduced.

Discussion

All organisms have to face harmful protein oxidation and almost all possess canonical Msrs that protect proteins by reducing MetO. Bacteria also have molybdoenzymes able to reduce MetO, as a free amino acid for the DMSO reductase [26] or the biotin sulfoxide reductase BisC/Z [24,25], but also included in proteins in the case of MsrP [28,29]. Genetic studies and the conservation of MsrP in most gram-negative bacteria indicate that it is very likely a key player in the protection of periplasmic proteins against oxidative stress [28,29] However, an in-depth characterization of its protein substrate specificity is still lacking. In this work, we chose the MsrP from the photosynthetic purple bacteria *R. sphaeroides* as a model enzyme to uncover such specificity. Using purified oxidized proteins and peptides, we showed that RsMsrP is a very efficient protein-containing MetO reductase, with apparent affinities (K_m) for oxidized proteins 10 to 100-fold lower than for the tripeptide Ser-MetO-Ser or the free MetO (Table 1). As reported for canonical MsrA and MsrB [15], we observed important variations in the reduction k_{cat} of different oxidized proteins, arguing for the existence of sequence and structural determinants affecting the enzyme efficiency (Table 1).

To find potential physiological substrates of RsMsrP and uncover their properties, we used a proteomic approach aiming at comparing the oxidation state of periplasmic proteins after treatment with the strong oxidant NaOCl, followed by RsMsrP reduction of these proteins. We found 202 unique Met, belonging to 70 proteins, for which the sensitivity of oxidation and the ability to serve as an RsMsrP substrate varied greatly (Figure 3, Supplementary Table S2). MetO efficiently reduced by RsMsrP belong to structurally and functionally unrelated proteins, indicating that RsMsrP very likely does not possess specific substrates and acts as a global protector of protein integrity in the periplasm. Interestingly, we observed from our IceLogo analysis that Met sensitive to oxidation are generally presented in a polar amino acid environment and can be found in clusters (Figure 4). These properties might be common to all Met in proteins as similar results were found in human cells [41,42] and plants [43]. Moreover, oxidized Met efficiently reduced by the RsMsrP were also found clustered in polar environments and our analysis shows that the presence of Thr and Pro in N-terminal side of a MetO strongly decrease RsMsrP efficiency (Table 1, Figure 5 and

503 Supplementary Figure S6). To our knowledge, the presence of a Thr close to a MetO was not previously
504 shown to influence any Msr activity, but the presence of a Pro was shown to decrease or totally inhibit MetO
505 reduction by the human MsrA and MsrB3, depending on its position [41].

506 The presence of oxidation-sensitive Met efficiently reduced by the RsMsrP in clusters on polar parts of
507 proteins should facilitate the oxidation/reduction cycle aiming to scavenge ROS as previously proposed for
508 canonical Msrs [44]. This is also illustrated by the methionine-rich protein MrpX proposed as main substrate
509 of the *A. suillum* MsrP, which is almost only composed of Met, Lys, Glu and Asp [29]. The presence of
510 numerous MetO on a single molecule of protein substrate should increase the RsMsrP efficiency as one
511 molecule of the substrate allows several catalytic cycles, potentially without breaking physical contact
512 between the enzyme and its substrate.

513 Comparison of the RsMsrP activity using folded or unfolded protein substrates (lysozyme and GST)
514 showed that it is far more efficient to reduce unfolded oxidized proteins (Figure 6). Similar results were
515 found for canonical Msrs [15]. In the case of MsrB it was because more MetO were accessible for reduction
516 whereas for MsrA this increase was independent of the number of MetO reduced. Here, the use of lysozyme
517 containing only one MetO (Supplementary Figure S7) undoubtedly showed that the increase in activity is
518 not related to the unmasking of additional MetO upon protein denaturation (Table 1; Figure 6). This could
519 indicate that the RsMsrP has better access to the MetO in the protein or that the MetO is more easily
520 accommodated in the active site of the enzyme because of increased flexibility. This should provide a
521 physiological advantage to the bacteria during oxidative attacks, which could occur during other stresses
522 such as acid or heat, hence promoting simultaneous oxidation and unfolding of proteins. Particularly,
523 hypochlorous acid, which was shown to induce *msrP* expression in *E. coli* [28] and *A. suillum* [29], has
524 strong oxidative and unfolding effect on target proteins [45].

525 Finally, previous work indicated that the *E. coli* MsrP lacks stereospecificity and can reduce both *R*- and
526 *S*-diastereomers of MetO chemically isolated from a racemic mixture of free L-Met-*R,S*-O [28]. This
527 discovery is of fundamental importance as it breaks a paradigm in Met oxidation and reduction knowledge,

and very likely for all enzymology as non-stereospecific enzymes were very rarely described. Indeed, to our knowledge, all previously characterized enzymes able to reduce Met sulfoxide or related substrates were shown to be absolutely stereospecific. This was the case for the canonical MsrA and MsrB, which reduce only the *S*-diastereomer and the *R*-diastereomer, respectively [7,9–14], as well as for the free Met-*R*-O reductase [22,23] and for the DMSO reductase [26,27] and BisC/Z molybdoenzymes [24,25]. To evaluate the potential lack of stereospecificity of the RsMsrP, we chose to use a different strategy than the one used for *E. coli* MsrP [28] and prepared oxidized β-casein containing only one or the other MetO diastereomer using yeast MsrA and MsrB to eliminate the *S*- and the *R*-diastereomers, respectively. Activity assays and kinetic experiments using a highly purified RsMsrP demonstrated that it can efficiently reduce the β-casein containing only the *R*- or the *S*-diastereomer (Table 1; Figure 2 and Supplementary Figure S4). Moreover, this lack of stereospecificity was undoubtedly confirmed by the ability of the RsMsrP to reduce all 6 MetO formed on the oxidized β-casein (Figure 1). These results, consistent with Gennaris and coworkers finding, indicate that this lack of stereospecificity is very likely common to all MsrP homologs. Together with the apparent ability of the enzyme to repair numerous unrelated oxidized proteins, the capacity to reduce both diastereomers of MetO, argues for a role of MsrP in the general protection of envelope integrity in gram negative bacteria. However, it raises questions regarding the structure of its active site as the enzyme should be able to accommodate both diastereomers. From this, we wondered whether the RsMsrP could reduce the Met sulfone, which can be imagined as a form of oxidized Met containing both *R*- and *S*-diastereomers, but we did not detect any activity (Supplementary Figure S9). Although it could be because of an incompatibility in redox potential, it may indicate that this form of oxidized Met cannot reach the catalytic atom. The three-dimensional structure of the oxidized form of *E. coli* MsrP indicated that the molybdenum atom, which is supposed to be the catalytic center of the enzyme, is buried 16 Å from the surface of the protein [46]. The next challenge will be to understand the MsrP reaction mechanism and will require the determination of the enzyme structure in its oxidized and reduced forms bound to its MetO-containing substrates.

Acknowledgment: We are very grateful to Prof. Vadim, N. Gladyshev (Brigham's and Women Hospital and Harvard Medical School) for the gift of pET28a-MsrA, pET21b-MsrB, pET15b-TR1, pET15b-Trx1 and pGEX4T1 expression vectors. We thank Dr. Benjamin Ezraty and the members of his team (Laboratoire de Chimie Bactérienne, Institut de Microbiologie de la Méditerranée) for fruitful discussions. Pascaline Auroy-Tarrago (Laboratoire de Bioénergétique et Biotechnologie des Bactéries et Microalgues, CEA, BIAM) is acknowledged for her help with proteomics analysis.

Competing Interests: The Authors declare that there are no competing interests associated with the manuscript.

Funding: This work was supported by the Commissariat à l'Energie Atomique et aux Energies Alternatives (CEA) and by the project METOXIC (ANR 16-CE11-0012).

Author contribution: LT, PA, DP and MS designed the study. LT, SG, MIS and MS purified RsMsrP. LT and MS prepared all other proteins. LT, SG, MIS, MS performed biochemical characterization of RsMsrP. LT, MS and DL performed β-casein and lysozyme mass spectrometry analysis and analyzed the data. SG and MS prepared *R. sphaeroides* 2.4.1 *msrP*$^{-}$ mutant and periplasmic proteins samples. BA, GM and JA performed proteomics analysis of periplasmic proteins and LT, MS, GM and JA analyzed the data. LT wrote the manuscript with contribution of MIS, DL, PA, DP, JA and MS. All authors approved the final manuscript.

References

1 Messner, K. R. and Imlay, J. A. (1999) The identification of primary sites of superoxide and hydrogen peroxide formation in the aerobic respiratory chain and sulfite reductase complex of Escherichia coli. J. Biol. Chem. **274**, 10119–10128.

2 Glaeser, J., Nuss, A. M., Berghoff, B. A. and Klug, G. (2011) Singlet oxygen stress in microorganisms. Adv. Microb. Physiol. **58**, 141–173.

3 Ezraty, B., Gennaris, A., Barras, F. and Collet, J.-F. (2017) Oxidative stress, protein damage and repair in bacteria. Nat. Rev. Microbiol. **15**, 385–396.

4 Imlay, J. A. (2013) The molecular mechanisms and physiological consequences of oxidative stress: lessons from a model bacterium. Nat. Rev. Microbiol. **11**, 443–454.

5 Ziegelhoffer, E. C. and Donohue, T. J. (2009) Bacterial responses to photo-oxidative stress. Nat. Rev. Microbiol. **7**, 856–863.

6 Davies, M. J. (2005) The oxidative environment and protein damage. Biochim. Biophys. Acta **1703**, 93–109.

7 Sharov, V. S., Ferrington, D. A., Squier, T. C. and Schöneich, C. (1999) Diastereoselective reduction of protein-bound methionine sulfoxide by methionine sulfoxide reductase. FEBS Lett. **455**, 247–250.

8 Vogt, W. (1995) Oxidation of methionyl residues in proteins: tools, targets, and reversal. Free Radic. Biol. Med. **18**, 93–105.

9 Ejiri, S. I., Weissbach, H. and Brot, N. (1979) Reduction of methionine sulfoxide to methionine by Escherichia coli. J. Bacteriol. **139**, 161–164.

10 Lowther, W. T., Weissbach, H., Etienne, F., Brot, N. and Matthews, B. W. (2002) The mirrored methionine sulfoxide reductases of Neisseria gonorrhoeae pilB. Nat. Struct. Biol. **9**, 348–352.

11 Moskovitz, J., Singh, V. K., Requena, J., Wilkinson, B. J., Jayaswal, R. K. and Stadtman, E. R. (2002) Purification and characterization of methionine sulfoxide reductases from mouse and Staphylococcus aureus and their substrate stereospecificity. Biochem. Biophys. Res. Commun. **290**, 62–65.

12 Vieira Dos Santos, C., Cuiné, S., Rouhier, N. and Rey, P. (2005) The Arabidopsis plastidic methionine sulfoxide reductase B proteins. Sequence and activity characteristics, comparison of the expression with plastidic methionine sulfoxide reductase A, and induction by photooxidative stress. Plant Physiol. **138**, 909–922.

13 Grimaud, R., Ezraty, B., Mitchell, J. K., Lafitte, D., Briand, C., Derrick, P. J. and Barras, F. (2001) Repair of oxidized proteins. Identification of a new methionine sulfoxide reductase. J. Biol. Chem. **276**, 48915–48920.

14 Kumar, R. A., Koc, A., Cerny, R. L. and Gladyshev, V. N. (2002) Reaction mechanism, evolutionary analysis, and role of zinc in Drosophila methionine-R-sulfoxide reductase. J. Biol. Chem. **277**, 37527–37535.

15 Tarrago, L., Kaya, A., Weerapana, E., Marino, S. M. and Gladyshev, V. N. (2012) Methionine sulfoxide reductases preferentially reduce unfolded oxidized proteins and protect cells from oxidative protein unfolding. J. Biol. Chem. **287**, 24448–24459.

16 Tarrago, L. and Gladyshev, V. N. (2012) Recharging oxidative protein repair: catalysis by methionine sulfoxide reductases towards their amino acid, protein, and model substrates. Biochem. Biokhimiia **77**, 1097–1107.

17 Kim, H.-Y. (2013) The methionine sulfoxide reduction system: selenium utilization and methionine sulfoxide reductase enzymes and their functions. Antioxid. Redox Signal. **19**, 958–969.
18 Châtelain, E., Satour, P., Laugier, E., Ly Vu, B., Payet, N., Rey, P. and Montrichard, F. (2013) Evidence for participation of the methionine sulfoxide reductase repair system in plant seed longevity. Proc. Natl. Acad. Sci. U. S. A. **110**, 3633–3638.
19 Laugier, E., Tarrago, L., Vieira Dos Santos, C., Eymery, F., Havaux, M. and Rey, P. (2010) Arabidopsis thaliana plastidial methionine sulfoxide reductases B, MSRBs, account for most leaf peptide MSR activity and are essential for growth under environmental constraints through a role in the preservation of photosystem antennae. Plant J. Cell Mol. Biol. **61**, 271–282.
20 Saleh, M., Bartual, S. G., Abdullah, M. R., Jensch, I., Asmat, T. M., Petruschka, L., Pribyl, T., Gellert, M., Lillig, C. H., Antelmann, H., et al. (2013) Molecular architecture of Streptococcus pneumoniae surface thioredoxin-fold lipoproteins crucial for extracellular oxidative stress resistance and maintenance of virulence. EMBO Mol. Med. **5**, 1852–1870.
21 Skaar, E. P., Tobiason, D. M., Quick, J., Judd, R. C., Weissbach, H., Etienne, F., Brot, N. and Seifert, H. S. (2002) The outer membrane localization of the Neisseria gonorrhoeae MsrA/B is involved in survival against reactive oxygen species. Proc. Natl. Acad. Sci. U. S. A. **99**, 10108–10113.
22 Le, D. T., Lee, B. C., Marino, S. M., Zhang, Y., Fomenko, D. E., Kaya, A., Hacioglu, E., Kwak, G.-H., Koc, A., Kim, H.-Y., et al. (2009) Functional analysis of free methionine-R-sulfoxide reductase from Saccharomyces cerevisiae. J. Biol. Chem. **284**, 4354–4364.
23 Lin, Z., Johnson, L. C., Weissbach, H., Brot, N., Lively, M. O. and Lowther, W. T. (2007) Free methionine-(R)-sulfoxide reductase from Escherichia coli reveals a new GAF domain function. Proc. Natl. Acad. Sci. U. S. A. **104**, 9597–9602.
24 Ezraty, B., Bos, J., Barras, F. and Aussel, L. (2005) Methionine sulfoxide reduction and assimilation in Escherichia coli: new role for the biotin sulfoxide reductase BisC. J. Bacteriol. **187**, 231–237.
25 Dhouib, R., Othman, D. S. M. P., Lin, V., Lai, X. J., Wijesinghe, H. G. S., Essilfie, A.-T., Davis, A., Nasreen, M., Bernhardt, P. V., Hansbro, P. M., et al. (2016) A Novel, Molybdenum-Containing Methionine Sulfoxide Reductase Supports Survival of Haemophilus influenzae in an In vivo Model of Infection. Front. Microbiol. **7**, 1743.
26 Weiner, J. H., MacIsaac, D. P., Bishop, R. E. and Bilous, P. T. (1988) Purification and properties of Escherichia coli dimethyl sulfoxide reductase, an iron-sulfur molybdoenzyme with broad substrate specificity. J. Bacteriol. **170**, 1505–1510.
27 Abo, M., Tachibana, M., Okubo, A. and Yamazaki, S. (1995) Enantioselective deoxygenation of alkyl aryl sulfoxides by DMSO reductase from Rhodobacter sphaeroides f.s. denitrificans. Bioorg. Med. Chem. **3**, 109–112.
28 Gennaris, A., Ezraty, B., Henry, C., Agrebi, R., Vergnes, A., Oheix, E., Bos, J., Leverrier, P., Espinosa, L., Szewczyk, J., et al. (2015) Repairing oxidized proteins in the bacterial envelope using respiratory chain electrons. Nature **528**, 409–412.
29 Melnyk, R. A., Youngblut, M. D., Clark, I. C., Carlson, H. K., Wetmore, K. M., Price, M. N., Iavarone, A. T., Deutschbauer, A. M., Arkin, A. P. and Coates, J. D. (2015) Novel mechanism for scavenging of hypochlorite involving a periplasmic methionine-rich Peptide and methionine sulfoxide reductase. mBio **6**, e00233-00215.
30 Juillan-Binard, C., Picciocchi, A., Andrieu, J.-P., Dupuy, J., Petit-Hartlein, I., Caux-Thang, C., Vivès, C., Nivière, V. and Fieschi, F. (2016) A two-component NOX-like system in

664 bacteria is involved in the electron transfer chain to the methionine sulfoxide reductase MsrP.
665 J. Biol. Chem.
666 31 Glaeser, J., Zobawa, M., Lottspeich, F. and Klug, G. (2007) Protein synthesis patterns reveal
667 a complex regulatory response to singlet oxygen in Rhodobacter. J. Proteome Res. **6**, 2460–
668 2471.
669 32 Sabaty, M., Grosse, S., Adryanczyk, G., Boiry, S., Biaso, F., Arnoux, P. and Pignol, D.
670 (2013) Detrimental effect of the 6 His C-terminal tag on YedY enzymatic activity and
671 influence of the TAT signal sequence on YedY synthesis. BMC Biochem. **14**, 28.
672 33 Prentki, P. and Krisch, H. M. (1984) In vitro insertional mutagenesis with a selectable DNA
673 fragment. Gene **29**, 303–313.
674 34 Quandt, J. and Hynes, M. F. (1993) Versatile suicide vectors which allow direct selection for
675 gene replacement in gram-negative bacteria. Gene **127**, 15–21.
676 35 Hartmann, E. M., Allain, F., Gaillard, J.-C., Pible, O. and Armengaud, J. (2014) Taking the
677 shortcut for high-throughput shotgun proteomic analysis of bacteria. Methods Mol. Biol.
678 Clifton NJ **1197**, 275–285.
679 36 Madeira, J.-P., Alpha-Bazin, B. M., Armengaud, J. and Duport, C. (2017) Methionine
680 Residues in Exoproteins and Their Recycling by Methionine Sulfoxide Reductase AB Serve
681 as an Antioxidant Strategy in Bacillus cereus. Front. Microbiol. **8**, 1342.
682 37 Klein, G., Mathé, C., Biola-Clier, M., Devineau, S., Drouineau, E., Hatem, E., Marichal, L.,
683 Alonso, B., Gaillard, J.-C., Lagniel, G., et al. (2016) RNA-binding proteins are a major target
684 of silica nanoparticles in cell extracts. Nanotoxicology **10**, 1555–1564.
685 38 Colaert, N., Helsens, K., Martens, L., Vandekerckhove, J. and Gevaert, K. (2009) Improved
686 visualization of protein consensus sequences by iceLogo. Nat. Methods **6**, 786–787.
687 39 Kim, Y. K., Shin, Y. J., Lee, W.-H., Kim, H.-Y. and Hwang, K. Y. (2009) Structural and
688 kinetic analysis of an MsrA-MsrB fusion protein from Streptococcus pneumoniae. Mol.
689 Microbiol. **72**, 699–709.
690 40 Ray, S. S., Singh, S. K. and Balaram, P. (2001) An electrospray ionization mass spectrometry
691 investigation of 1-anilino-8-naphthalene-sulfonate (ANS) binding to proteins. J. Am. Soc.
692 Mass Spectrom. **12**, 428–438.
693 41 Ghesquière, B., Jonckheere, V., Colaert, N., Van Durme, J., Timmerman, E., Goethals, M.,
694 Schymkowitz, J., Rousseau, F., Vandekerckhove, J. and Gevaert, K. (2011) Redox
695 proteomics of protein-bound methionine oxidation. Mol. Cell. Proteomics MCP **10**,
696 M110.006866.
697 42 Hsieh, Y.-J., Chien, K.-Y., Yang, I.-F., Lee, I.-N., Wu, C.-C., Huang, T.-Y. and Yu, J.-S.
698 (2017) Oxidation of protein-bound methionine in Photofrin-photodynamic therapy-treated
699 human tumor cells explored by methionine-containing peptide enrichment and quantitative
700 proteomics approach. Sci. Rep. **7**, 1370.
701 43 Jacques, S., Ghesquière, B., De Bock, P.-J., Demol, H., Wahni, K., Willems, P., Messens, J.,
702 Van Breusegem, F. and Gevaert, K. (2015) Protein Methionine Sulfoxide Dynamics in
703 Arabidopsis thaliana under Oxidative Stress. Mol. Cell. Proteomics MCP **14**, 1217–1229.
704 44 Luo, S. and Levine, R. L. (2009) Methionine in proteins defends against oxidative stress.
705 FASEB J. Off. Publ. Fed. Am. Soc. Exp. Biol. **23**, 464–472.
706 45 Winter, J., Ilbert, M., Graf, P. C. F., Ozcelik, D. and Jakob, U. (2008) Bleach activates a
707 redox-regulated chaperone by oxidative protein unfolding. Cell **135**, 691–701.
708 46 Loschi, L., Brokx, S. J., Hills, T. L., Zhang, G., Bertero, M. G., Lovering, A. L., Weiner, J.
709 H. and Strynadka, N. C. J. (2004) Structural and Biochemical Identification of a Novel
710 Bacterial Oxidoreductase. J. Biol. Chem. **279**, 50391–50400.

711 **Table**

712 **Table 1.** Kinetics parameters of RsMsrP reductase activity towards DMSO and various MetO-containing
713 substrates.

Substrates	k_{cat} (s^{-1})	K_m (µM)	k_{cat}/K_m ($M^{-1}.s^{-1}$)
DMSO[a]	28 ± 1	61,000 ± 7,000	465
Free L-Met-*R*,*S*-O	122 ± 20	115,000 ± 27,000	1,000
Ser-MetO-Ser	108 ± 17	13,000 ± 3,400	8,300
QWGAGM(O)QAEED	479 ± 24	4,530 ± 370	105,700
TTPGYM(O)EEWNK	> 70	> 5,000	N.D.
Oxidized β-casein	100 ± 5	93 ± 9	1,075,000
β-casein-*R*-O	49 ± 3	51 ± 6	950,000
β-casein-*S*-O	8 ± 1	53 ± 10	142,000
Oxidized lysozyme	4 ± 1	886 ± 349	4,000
Unfolded oxidized lysozyme	7 ± 1	105 ± 17	70,200
Oxidized GST	8 ± 2	643 ± 194	12,400
Unfolded oxidized GST	12 ± 3	99 ± 33	120,000

714 [a] From [32]. *N.D, not determined.*

715

Figures legends

Figure 1. Mass spectrometry spectrum of β-casein non-oxidized (A), oxidized with H_2O_2 (B) and repaired by RsMsrP (C). A) Commercial β-casein exists as a mixture of genetic variants (7 in our batch). β-casein was analyzed by ESI-MS. Main peaks masses: 1, 23982.7 Da; 2, 24021.6 Da; 3, 24035.9 Da; 4, 24075.0 Da; 5, 24089.1 Da; 6, 24127.5 Da; 7, 24142.5 Da. B) β-casein was oxidized with 50 mM H_2O_2 before MS analysis. All major peaks underwent an increase of ~ 96 Da compared to the non-oxidized sample. Main peaks masses: 1, 24079.1 Da; 2, 24118.5 Da; 3, 24131.8 Da; 4, 24172.2 Da; 5, 24184.3 Da; 6, 24224.4 Da; 7, 24238.2 Da. C) Oxidized β-casein was incubated with RsMsrP (25 nM) in the presence of BV (0.8 mM) and sodium dithionite (2 mM) as electron donors. All major peaks had masses corresponding of the non-oxidized β-casein, showing the ability to reduce all MetO in this protein. Note the presence of a peak with an increase of 16 Da (*, mass of 23999.4 Da) compared to the main reduced peak, indicating an incomplete reduction of the total protein pool. Main peaks masses: 1, 23983.0 Da; 2, 24022.4 Da; 3, 24037.1 Da; 4, 24075.0 Da; 5, 24091.0 Da; 6, 24128.2 Da; 7, 24143.7 Da.

Figure 2. RsMsrP activity using oxidized β-casein, β-casein-*R*-O and β-casein-*S*-O as substrates. The oxidized β-casein (100 µM) containing both diastereomers of MetO, only the *R* one ("*β-casein*-R-*O"*), or only the *S* one ("*β-casein*-S-*O*") were assayed as substrates of RsMsrP. The RsMsrP activity was determined using benzyl viologen (BV) (0.8 mM) as an electron provider in a glove box under nitrogen. BV was initially reduced with sodium dithionite (2 mM) and oxidation was followed at 600 nm after addition of the enzyme (30 nM). The reaction was done in 50 mM MES, pH6.0. The activity values presented as k_{cat} (s^{-1}) represent the number of mole of MetO reduced per mole of enzyme per second as 2 moles of BV is oxidized per mole of MetO reduced. Data presented are averages of 3 replicates. ± S.D.

Figure 3. Characteristics of MetO reduction sites and oxidation state of Met in representative proteins. A) Repartition of the number of MetO per percentage of reduction by RsMsrP. B) Percentage of oxidation of Met 353 of putative ABC transporter from HAAT family in the 3 analyzed samples. C) Percentage of oxidation of Met 230 and 243 of ABC transporter DdpA. D) Percentage of oxidation of Met

92, 172 and 190 in the peptidyl-prolyl cis-trans isomerase. E) Percentage of oxidation of Met 123, 438 and 539 of the pyrroloquinoline quinone (PQQ) dehydrogenase XoxF.

Figure 4. IceLogo representation of enriched and depleted amino acids around the sites of Met oxidation. A) Enrichment and depletion of amino acids around the oxidized Met (M) found in periplasmic extracts and oxidized periplasmic extracts by comparison with the theoretical proteome of *R. sphaeroides*. B) The same oxidized peptides were analyzed using the peptides containing a non-oxidized Met from the same samples (periplasm and oxidized periplasm extracts). Amino acids are colored according to their physiochemical properties.

Figure 5. IceLogo representation of enriched and depleted amino acids around the sites of MetO reduction by RsMsrP. A) Enrichment of amino acids in peptides centered on the MetO for which the percentage of reduction and the decrease in the percentage of oxidation were both superior to 50 % by comparison with the theoretical proteome of *R. sphaeroides*. B) Enrichment of amino acids from peptides centered on the MetO for which the percentage of reduction and the decrease in percentage were inferior to 10 % by comparison with the theoretical proteome of *R. sphaeroides*. C) Enrichment and depletion of amino acids from efficiently reduced MetO-containing peptides (dataset used in A)) by comparison with inefficiently reduced MetO-containing peptides (dataset used in B)). Amino acids are colored according to their physiochemical properties.

Figure 6. Relative RsMsrP activity using unfolded oxidized proteins. The RsMsrP activity was determined as described in Figure 2. Oxidized and unfolded oxidized lysozyme were incubated at 100 µM in 50 mM MES, pH 6.0. Initial turnover numbers were 0.65 ± 0.12 s^{-1} and 7.38 ± 0.23 s^{-1} with oxidized and unfolded oxidized lysozyme, respectively. Activity with oxidized and unfolded oxidized GST (75 µM) was determined similarly except that reaction buffer was 30 mM Tris-HCl, pH 8.0 because unfolded oxidized GST precipitated in 50 mM MES, pH 6.0. Initial turnover numbers were 0.86 ± 0.08 s^{-1} and 5.31 ± 0.39 s^{-1} with oxidized and unfolded oxidized GST, respectively. Data presented are averages of three replicates. ± S.D.

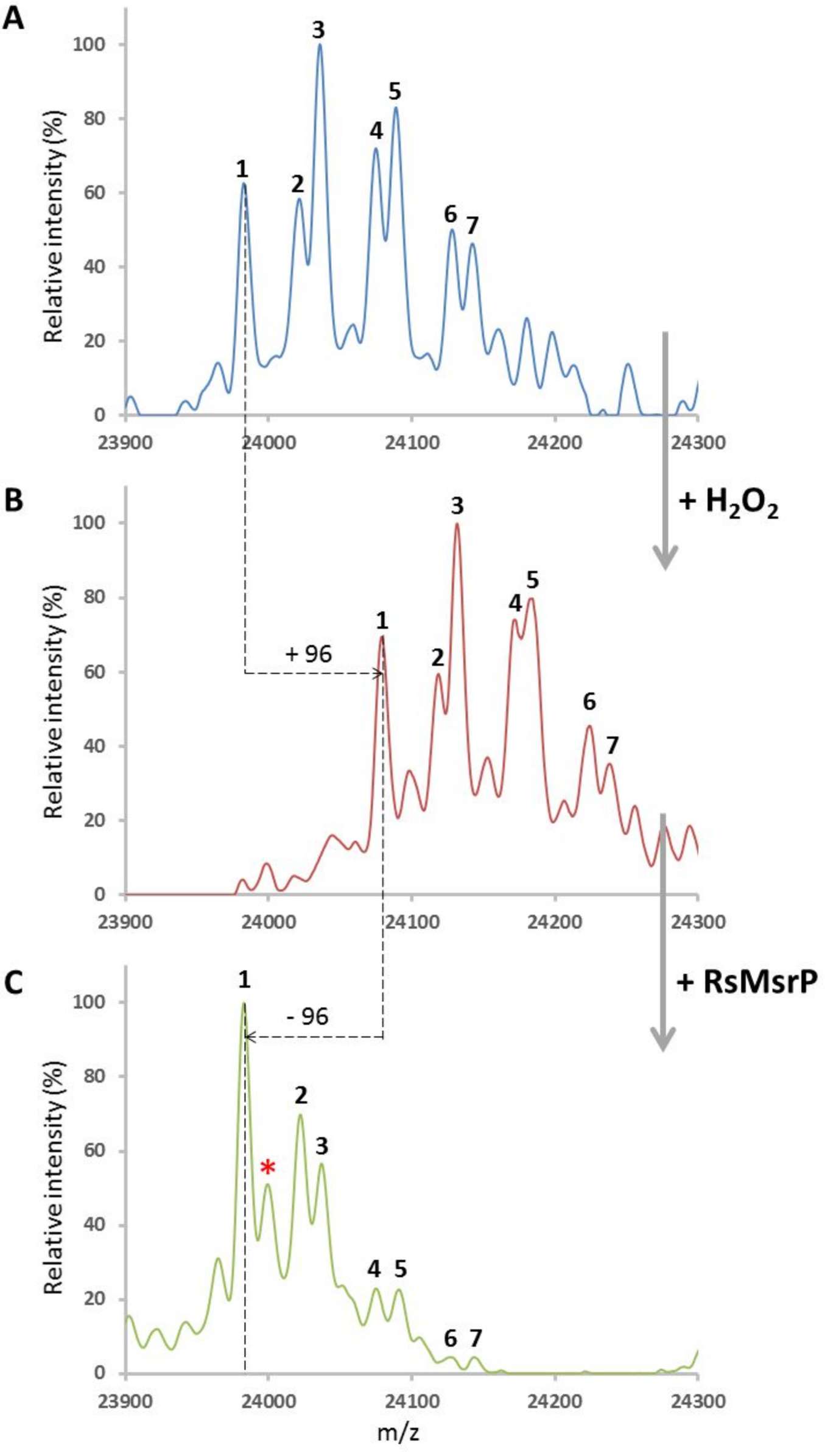
A
B
C
Relative intensity (%)
m/z
1
2
3
4
5
6
7
+ 96
- 96
*
+ H_2O_2
+ RsMsrP
0
20
40
60
80
100
23900
24000
24100
24200
24300

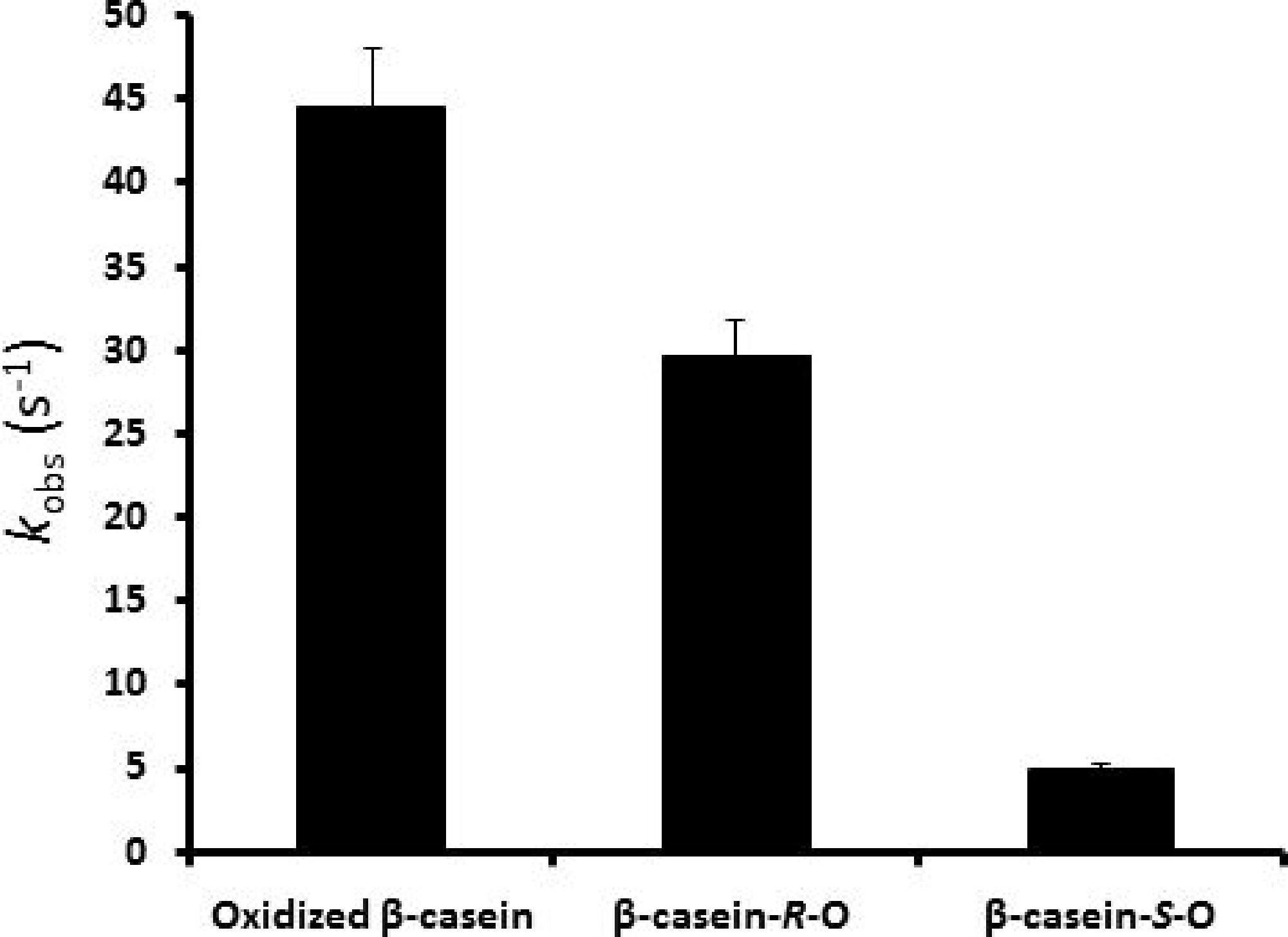
50
45
40
35
30
25
20
15
10
5
0
k_{obs} (s^{-1})
Oxidized β-casein
β-casein-*R*-O
β-casein-*S*-O

A

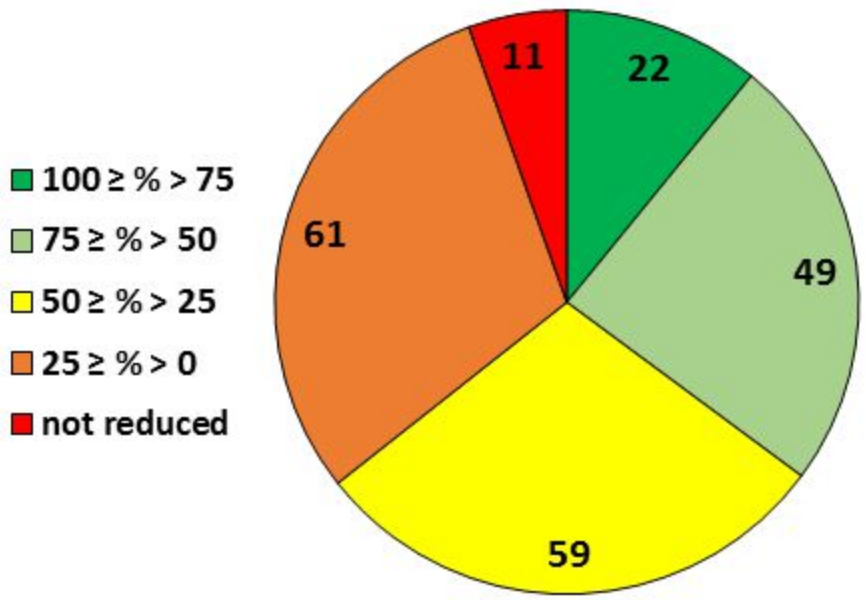
100 ≥ % > 75
75 ≥ % > 50
50 ≥ % > 25
25 ≥ % > 0
not reduced
22
49
59
61
11

B

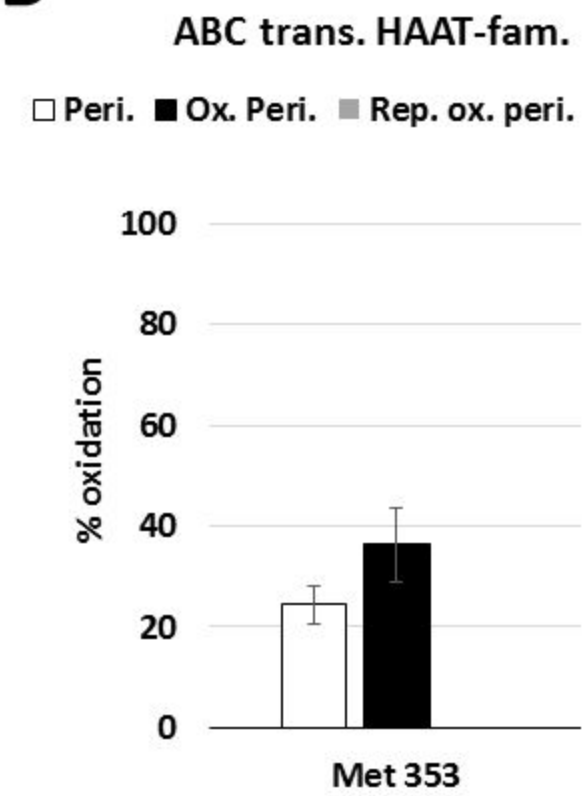
ABC trans. HAAT-fam.
Peri.
Ox. Peri.
Rep. ox. peri.
% oxidation
100
80
60
40
20
0
Met 353

C

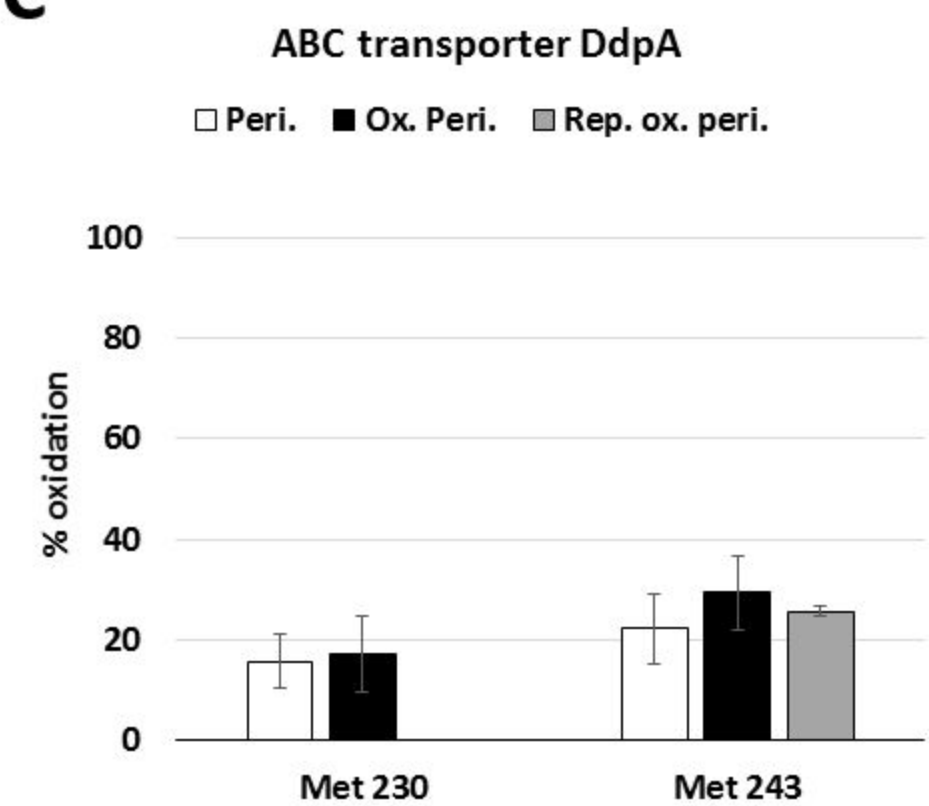
ABC transporter DdpA
Peri.
Ox. Peri.
Rep. ox. peri.
% oxidation
100
80
60
40
20
0
Met 230
Met 243

D

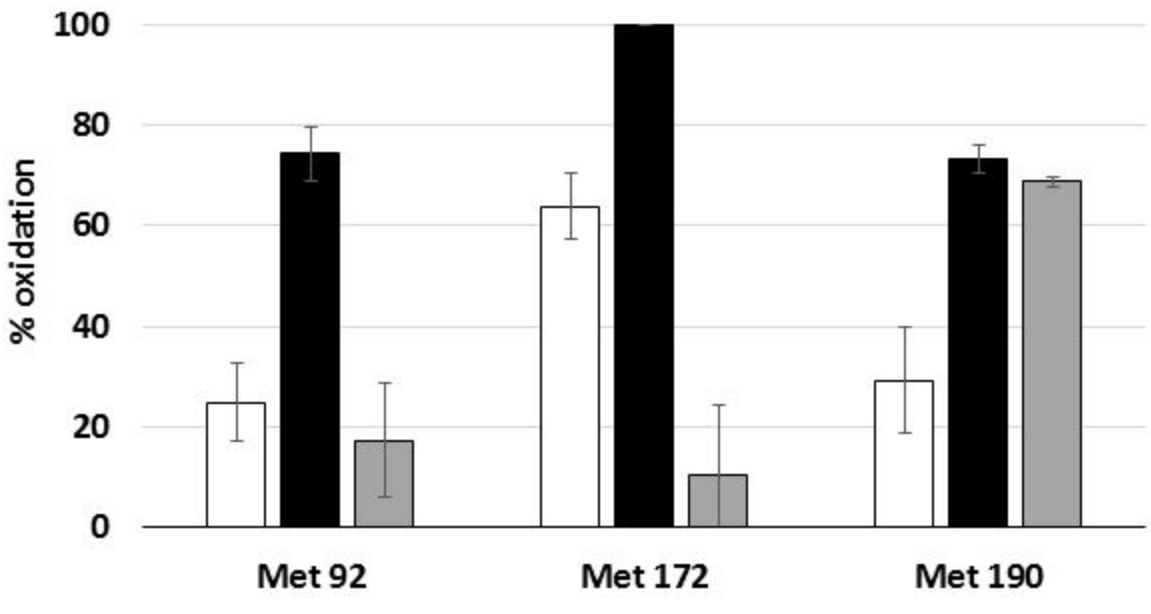
Peptidyl-prolyl cis-trans isomerase
Peri.
Ox. Peri.
Rep. ox. peri.
% oxidation
100
80
60
40
20
0
Met 92
Met 172
Met 190

E

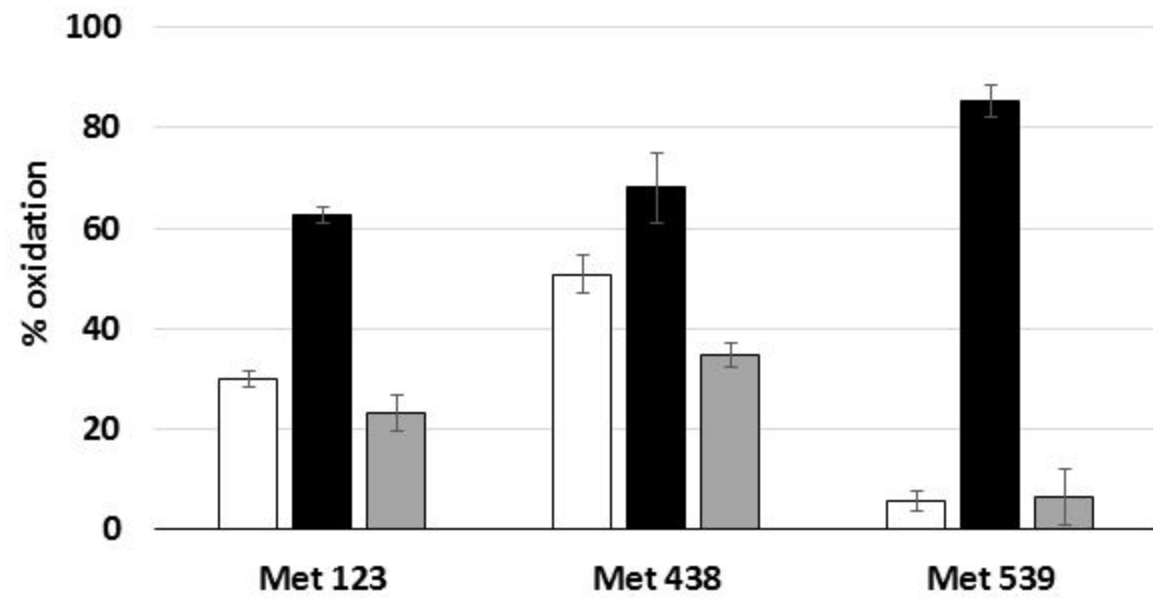
PQQ dehydrogenase XoxF
Peri.
Ox. Peri.
Rep. ox. peri.
% oxidation
100
80
60
40
20
0
Met 123
Met 438
Met 539

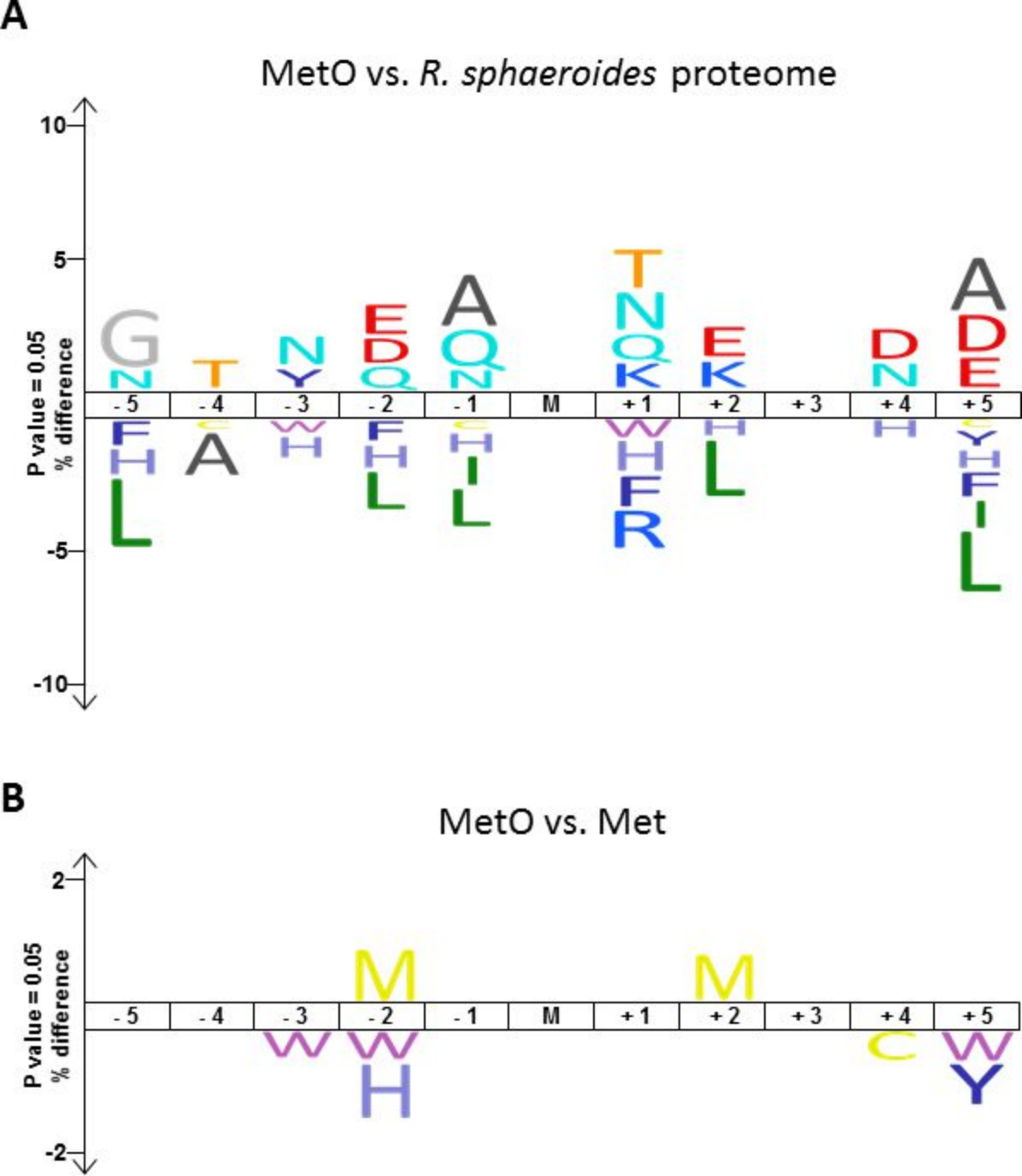
A
MetO vs. R. sphaeroides proteome
P value = 0.05
% difference
10
5
-5
-10
- 5
- 4
- 3
- 2
- 1
M
+ 1
+ 2
+ 3
+ 4
+ 5
B
MetO vs. Met
P value = 0.05
% difference
2
-2
- 5
- 4
- 3
- 2
- 1
M
+ 1
+ 2
+ 3
+ 4
+ 5

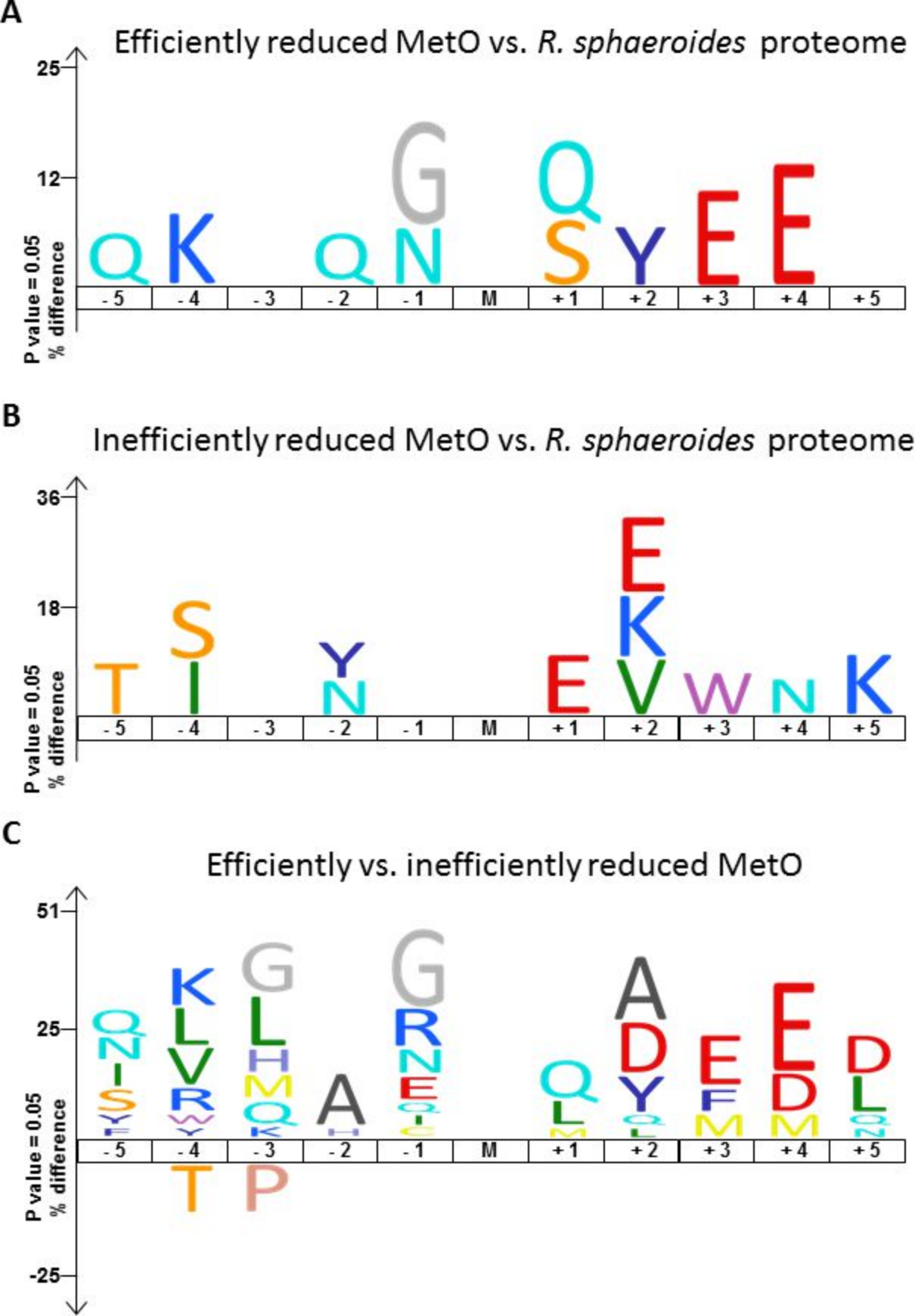
A
Efficiently reduced MetO vs. R. sphaeroides proteome
25
12
P value = 0.05
% difference
- 5
- 4
- 3
- 2
- 1
M
+ 1
+ 2
+ 3
+ 4
+ 5
B
Inefficiently reduced MetO vs. R. sphaeroides proteome
36
18
P value = 0.05
% difference
C
Efficiently vs. inefficiently reduced MetO
51
25
-25
P value = 0.05
% difference

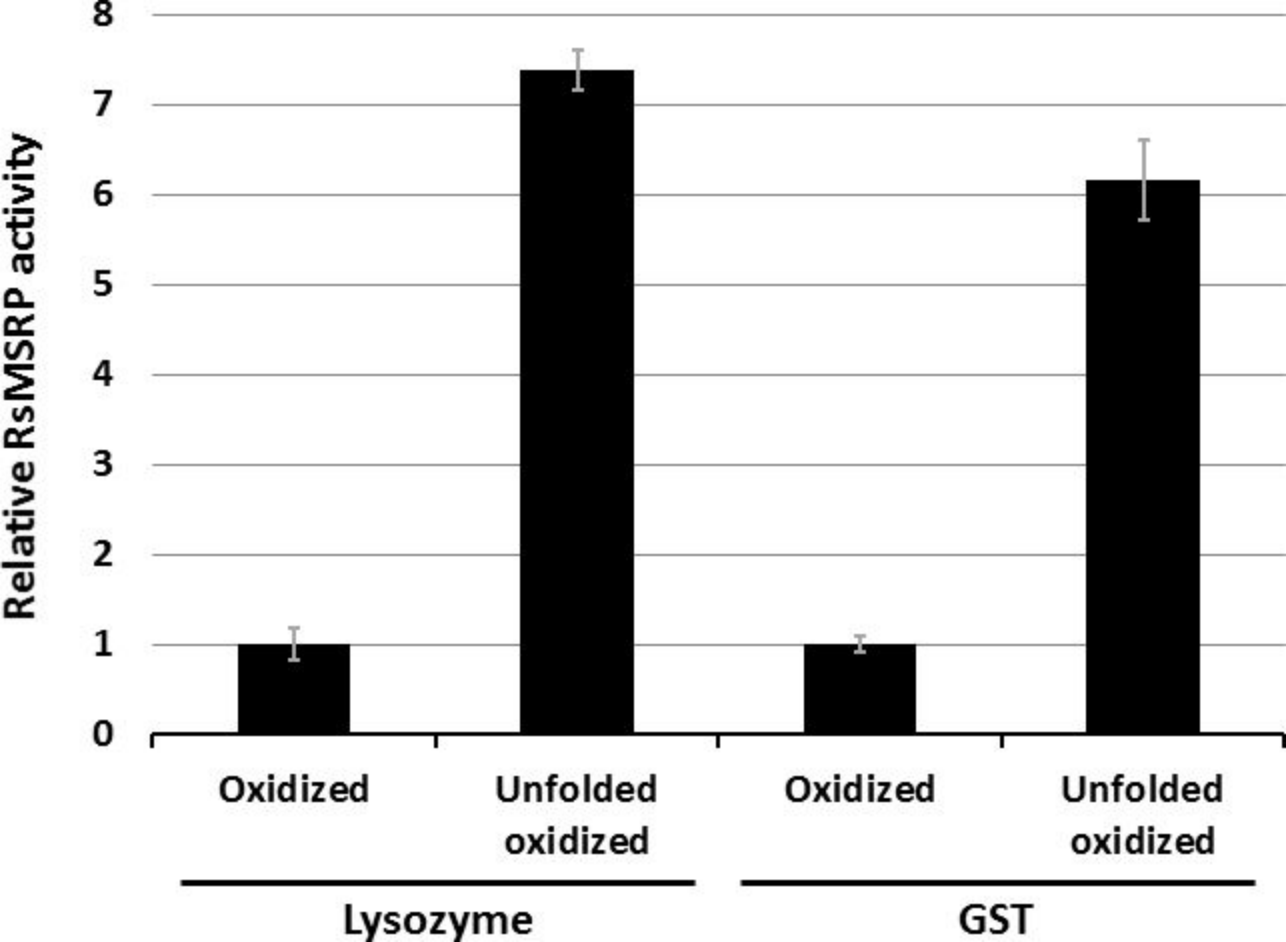
Relative RsMSRP activity
8
7
6
5
4
3
2
1
0
Oxidized
Unfolded oxidized
Oxidized
Unfolded oxidized
Lysozyme
GST